

Optical nanofiber as an efficient tool for manipulating and probing atomic fluorescence

K. P. Nayak,¹ P. N. Melentiev,^{1,3} M. Morinaga,² Fam Le Kien,¹
V. I. Balykin,^{1,3} and K. Hakuta^{1*}

¹*Department of Applied Physics and Chemistry, University of Electro-Communications,
Chofu, Tokyo 182-8585, Japan*

²*Institute for Laser Science, University of Electro-Communications,
Chofu, Tokyo 182-8585, Japan*

³*Institute of Spectroscopy, Troitsk, Moscow Region, 142190, Russia*

*Corresponding author: hakuta@pc.uec.ac.jp

Abstract: We experimentally demonstrate efficient coupling of atomic fluorescence to the guided mode of a subwavelength-diameter silica fiber, an optical nanofiber. We show that fluorescence of a very small number of atoms, around the nanofiber can be readily observed through a single-mode optical fiber. We also show that such a technique enables us to probe the van der Waals interaction between atoms and surface with high precision by observing the fluorescence excitation spectrum through the nanofiber.

© 2007 Optical Society of America

OCIS codes: (270.0270) Quantum optics; (020.0020) Atomic and molecular physics; (300.6210) Spectroscopy, atomic; (240.6490) Spectroscopy, surface.

References and links

1. L. Tong, R. R. Gattass, J. B. Ashcom, S. He, J. Lou, M. Shen, I. Maxwell, and E. Mazur, "Subwavelength-diameter silica wires for low-loss optical wave guiding," *Nature (London)* **426**, 816-819 (2003).
2. S. G. Leon-Saval, T. A. Birks, W. J. Wadsworth, and P. St. J. Russell, "Supercontinuum generation in submicron fibre waveguides," *Opt. Express* **12**, 2864-2869 (2004).
3. M. Sumetsky, Y. Dulashko, and A. Hale, "Fabrication and study of bent and coiled free silica nanowires: Self-coupling microloop optical interferometer," *Opt. Express* **12**, 3521-3531 (2004).
4. M. Sumetsky, Y. Dulashko, J. M. Fini, A. Hale, and D. J. DiGiovanni, "The Microfiber Loop Resonator: Theory, Experiment, and Application," *J. Lightwave Technol.* **24**, 242-250 (2006).
5. Fam Le Kien, S. Dutta Gupta, V. I. Balykin, and K. Hakuta, "Spontaneous emission of a cesium atom near a nanofiber: Efficient coupling of light to guided modes," *Phys. Rev. A* **72**, 032509 (2005).
6. Fam Le Kien, S. Dutta Gupta, K. P. Nayak, and K. Hakuta, "Nanofiber-mediated radiative transfer between two distant atoms," *Phys. Rev. A* **72**, 063815 (2005).
7. V. I. Balykin, K. Hakuta, Fam Le Kien, J. Q. Liang, and M. Morinaga, "Atom trapping and guiding with a subwavelength-diameter optical fiber," *Phys. Rev. A* **70**, 011401(R) (2004).
8. Fam Le Kien, V. I. Balykin, and K. Hakuta, "Atom trap and waveguide using a two-color evanescent light field around a subwavelength-diameter optical fiber," *Phys. Rev. A* **70**, 063403 (2004).
9. M. Sumetsky, "How thin can a microfiber be and still guide light?," *Opt. Lett.* **31**, 870-872 (2006).
10. M. Oriá, M. Chevrollier, D. Bloch, M. Fichet, and M. Ducloy, "Spectral observation of surface-induced van der Waals attraction on atomic vapor," *Europhys. Lett.* **14**, 527-532 (1991).
11. M. Chevrollier, M. Chevrollier, D. Bloch, G. Rahmat, and M. Ducloy, "Van der Waals-induced spectral distortions in selective-reflection spectroscopy of Cs vapor: the strong atom-surface interaction regime," *Opt. Lett.* **16**, 1879-1881 (1991).
12. W. R. Johnson, V. A. Dzuba, and U. I. Safronova, "Finite-field evaluation of the Lennard-Jones atom-wall interaction constant C_3 for alkali-metal atoms," *Phys. Rev. A* **69**, 022508 (2004).
13. Fam Le Kien, S. Dutta Gupta, and K. Hakuta, "Optical excitation spectrum of an atom in a surface-induced potential," *Phys. Rev. A* **75**, 032508 (2007).

14. Fam Le Kien and K. Hakuta, "Spontaneous radiative decay of translational levels of an atom near a dielectric surface," *Phys. Rev. A* **75**, 013423 (2007).
 15. E. G. Lima, M. Chevrollier, O. Di Lorenzo, P. C. Segundo, and M. Oriá, "Long-range atom-surface bound states," *Phys. Rev. A* **62**, 013410 (2000).
 16. T. Passerat de Silans, B. Farias, M. Oriá, and M. Chevrollier, "Laser-induced quantum adsorption of neutral atoms in dielectric surfaces," *Appl. Phys. B* **82**, 367-371 (2006).
 17. D. A. Braje, V. Balić, S. Goda, G. Y. Yin, and S. E. Harris, "Frequency Mixing Using Electromagnetically Induced Transparency in Cold Atoms," *Phys. Rev. Lett.* **93**, 183601 (2004).
 18. V. Balić, D. A. Braje, P. Kolchin, G. Y. Yin, and S. E. Harris, "Generation of Paired Photons with Controllable Waveforms," *Phys. Rev. Lett.* **94**, 183601 (2005).
 19. A. T. Black, J. K. Thompson, and Vladan Vuletić, "On-Demand Superradiant Conversion of Atomic Spin Gratings into Single Photons with High Efficiency," *Phys. Rev. Lett.* **95**, 133601 (2005).
-

1. Introduction

Recently, thin optical fibers with subwavelength diameters, termed as optical nanofibers, have attracted considerable attentions. Tong *et al.* developed a method to fabricate optical nanofibers with diameters down to 50 nm and demonstrated a wide range of possible photonic applications like low loss optical waveguiding [1]. Leon-Saval *et al.* demonstrated supercontinuum generation using a unique property of propagating field confinement of nanofibers [2]. Sumetsky *et al.* demonstrated a new type of optical resonator, micro-ring resonator, using evanescent coupling between nanofiber coils [3, 4].

From a viewpoint of quantum optics, optical nanofiber may become a fascinating work bench due to the possibility of the quantum electrodynamic (QED) effects associated with the confinement of the field in the guided mode. It has been theoretically demonstrated that spontaneous emission of atoms can be strongly enhanced around the nanofiber and an appreciable amount of fluorescence photons can be channeled into a single guided mode of the nanofiber [5]. Furthermore, two distant atoms on the nanofiber surface can be entangled through the guided mode [6]. Novel atom trapping schemes, using optical nanofiber, are also proposed [7, 8]. These possibilities may open new approaches for manipulating a single atom or a single photon, which will offer new tools for quantum information technology.

In the present work we experimentally demonstrate how optical nanofibers can work for manipulating and probing atomic fluorescence. We use laser-cooled Cs-atoms to realize interaction time longer than the atomic spontaneous emission lifetime. We show that fluorescence photons from a very small number of atoms around the nanofiber can be measured efficiently through the fiber guided mode. We also show that, due to the inherent nature of the nanofiber method, the fluorescence excitation spectrum strongly reflects the effect of the van der Waals interaction between atoms and nanofiber surface.

In Section 2 we describe the experimental arrangements and techniques. In Section 3 we discuss the measurement of fluorescence of MOT atoms through the nanofiber. In Section 4 we discuss the measurement of fluorescence of cold atoms using a separate probe beam. In Section 5 we discuss the measurement of fluorescence excitation spectrum through the nanofiber. Finally in Section 6 we summarize the results of the present work discussing wide range of possible applications.

2. Experimental Setup

Figure 1(a) shows the conceptual diagram of the present experiment. The nanofiber locates at the mid of a tapered optical fiber. A key point is the adiabatic tapering of a single mode optical fiber so that the single-mode propagation condition can be maintained for the whole fiber length [9]. Fluorescence photons emitted into the guided mode are measured through the optical fiber. Figure 1(b) shows the coupling efficiency of spontaneous emission into each direction of the

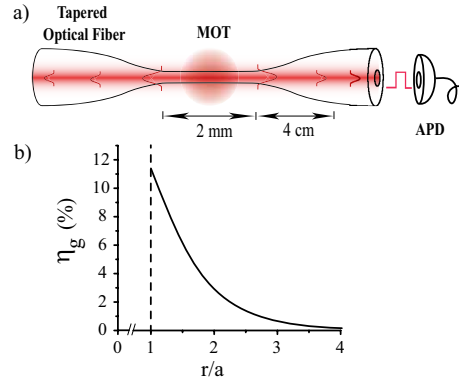


Fig. 1. (a) Conceptual diagram of the experiment. Optical nanofiber locates at the mid of tapered optical fiber. APD denotes avalanche photodiode. (b) Coupling efficiency of spontaneous emission into each direction of nanofiber propagation mode, η_g , versus atom position r/a , where r and a are distance from nanofiber axis and radius of nanofiber, respectively.

nanofiber fundamental-mode, in the evanescent region, that is theoretically calculated, based on Ref. [5], for a nanofiber with $k_0a = 1.45$, where k_0 is the free-space propagation constant and a is the radius of the nanofiber. Condition of $k_0a = 1.45$ is the optimum condition for coupling the fluorescence into the guided mode. One can see that the nanofiber can collect fluorescence photons very efficiently. For atoms on the nanofiber surface, 11 % of the fluorescence photons are channelled into each side of the guided mode, and for atoms at one radius away from the surface it is still 3 %.

We make tapered fibers, by heating and pulling commercial single-mode optical fibers with cut-off wavelength of 780 nm, using a fiber-coupler production system (NTT-AT, FCI-7011). The length of the tapered region is 4 cm on either side, which ensures adiabatic tapering condition. Using this system, we make optical nanofibers with diameters from 100 to 1,000 nm. Diameters are measured by a scanning electron microscope. The diameters are uniform for 2 mm along the length. Regarding the surface roughness, we have not seen any irregularities within a resolution of 30 nm. For the present experiments, we use nanofibers with diameter of 400 nm, which satisfy the condition of $k_0a = 1.45$ for the D2 transition of Cs-atom.

One of the obstructions in maintaining high-transmission properties of the optical nanofiber, is dust in the air. The problem of dust is minimized by placing the whole manufacturing unit inside a clean box and maintaining a flux of filtered air inside the box. By carrying out preparation of nanofibers under such clean conditions, high transmission of 87 % is realized. After the preparation, we install the nanofiber into the vacuum chamber. The vacuum chamber is filled with dust free Ar-gas and the nanofiber is installed horizontally into the chamber through a flange. Although the flux of Ar-gas is maintained during the installation procedure, the loss increases during the installation and the measured transmission T_0 after installation is typically 40 %.

We use a conventional magneto-optical trap (MOT) for cold Cs-atoms. The cooling laser is detuned 10 MHz below the closed cycle transition ($6S_{1/2}F = 4 \leftrightarrow 6P_{3/2}F' = 5$). Each cooling and repumping beam has an intensity of 3.3 mW/cm^2 with a beam diameter of 2 cm. The MOT has a number density of $2 \times 10^{10} \text{ atoms/cm}^3$ and the temperature of trapped atoms is 200 μK . The MOT is monitored by a CCD camera during the experiments. The MOT shape is elliptical with horizontal length of 2 mm and vertical length of 1 mm. The position of MOT

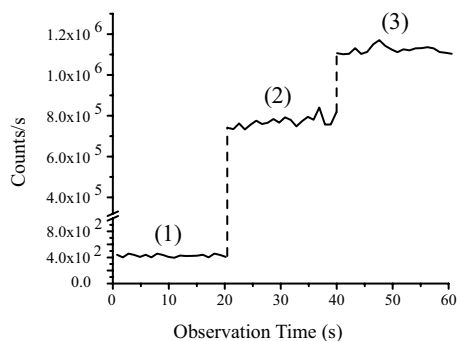


Fig. 2. Photon count through the optical fiber under three conditions; (1) both MOT laser beams and B-fields are switched off, (2) MOT laser beams are switched on, and (3) both MOT laser beams and B-fields are switched on.

is controlled by 2 mm in x, y and z -directions using the MOT quadrupole coils and other two pairs of Helmholtz coils. After installing the nanofiber into the chamber, the MOT is spatially overlapped with the nanofiber part of the tapered fiber using the 3 pairs of coils. By overlapping the MOT with the nanofiber, the MOT density is reduced to 0.7×10^{10} atoms/cm³, one third of the off-fiber value, and the temperature of atoms is raised to 400 μ K.

3. Measurement of fluorescence of MOT atoms through the nanofiber

First, we observe the fluorescence of MOT atoms around the nanofiber. Fluorescence photons are measured by using an avalanche photodiode (Perkin Elmer, SPCM-AQR/FC) connected to one end of the fiber. Signals are accumulated and recorded on a PC using a photon-counting PC-board (Hamamatsu, M8784). The observed photon counts are plotted in Fig. 2 for three conditions. During the first 20 seconds of observation both MOT beams and MOT magnetic fields are switched off and the observed 400 counts/s is due to room-light scattering and dark counts of the detector. For the next 20 seconds, MOT beams are switched on and the observed 8×10^5 counts/s corresponds to scattered light from MOT laser beams coupled to the guided mode of nanofiber. For the final 20 seconds, the MOT magnetic fields are switched on and the MOT is overlapped with the nanofiber. An increase of 3×10^5 counts/s above the scattering background is clearly observed.

The fluorescence photon count n_p is estimated as $n_p = NR\eta_{fiber}T\eta_D$, where N is the effective number of atoms, R the atomic scattering rate, η_{fiber} the averaged coupling efficiency of spontaneous emission to the guided mode, $T(= \sqrt{T_0})$ the fiber transmission from the mid to the one end, and η_D the detector quantum efficiency. T and η_D are 65 % and 45 %, respectively. Assuming an effective observation volume around the nanofiber of 200 nm thick hollow cylinder with 2 mm length, N and η_{fiber} are estimated as $N \approx 5$ and $\eta_{fiber} \approx 6$ %, respectively. For the total laser intensity of 6×3.3 mW/cm² and the detuning of 10 MHz, the atomic scattering rate is calculated to be 6.8×10^6 s⁻¹, with a saturation intensity of 2.5 mW/cm². For the above calculation we use an effective spontaneous emission rate of 3.6×10^7 s⁻¹ which includes the QED-enhancement factor [5]. Thus, we obtain the fluorescence photon count $n_p \approx 6.0 \times 10^5$ counts/s, which reasonably agrees with the observed value.

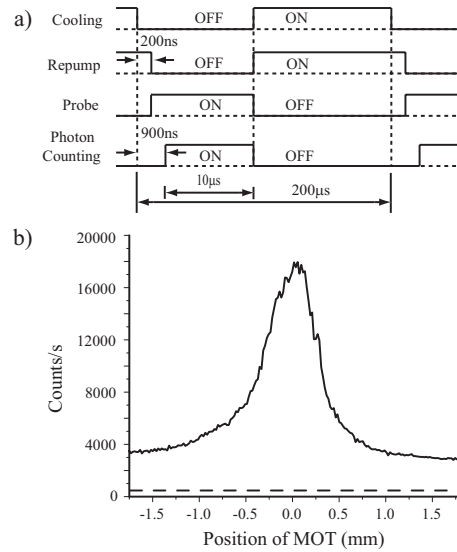


Fig. 3. (a) Time sequence for the measurements using probe laser. (b) Observed photon count versus MOT-position. Dashed line denotes the background count when the probe laser is off.

4. Measurement of fluorescence of cold atoms using a probe beam

Next, we discuss the cold atom fluorescence measurements with a probe laser beam. The observations are performed following the time sequence shown in Fig. 3(a). When the MOT has become ready, the cooling beam is switched off first, and the repumping beam is switched off 200 ns later, so that all the atoms can be optically pumped into the $F = 4$ hyperfine ground state. After switching off the repumping beam, the probe beam is switched on and the photon counting is started. The time interval between cooling-beam-off and photon-counting-on is 900 ns. The probe beam is irradiated perpendicularly to the nanofiber, in a standing wave configuration to minimize the resonant photon kick on the atoms, and the beam diameter is chosen to be 2 mm, just covering all the MOT atoms and the uniform nanofiber region. The polarization of the probe is linear and is perpendicular to the nanofiber axis. Photons are counted for 10 μ s. Then again the probe beam is switched off and the MOT beams are switched on for 190 μ s to recollect atoms into the MOT. In this way the observation is repeated at a rate of 5 kHz and the photon counts are accumulated for many cycles.

Figure 3(b) shows the observed photon count as a function of the MOT position with respect to the nanofiber. MOT position is scanned across the nanofiber in the vertical direction. The probe laser frequency is tuned to the resonance of $F = 4 \leftrightarrow 5$ transition and the laser intensity is 3.3 mW/cm². It is readily seen that the scattering background has been greatly reduced compared to the value when the MOT beams are on; the value is 2.5×10^3 counts/s. The spatial profile of the MOT is clearly observed with a good S/N ratio. The observed profile is slightly asymmetric. We have fitted the profile with a Gaussian profile and obtained $1/e^2$ -diameter of 1.1 mm which well corresponds to the value of CCD measurement.

Regarding the observed fluorescence-photon count, the peak value is 1.5×10^4 counts/s, which is about 1/20-times of that for the MOT observation in Fig. 2. We estimate the average number of atoms in the observation volume from the peak value using the same relation $n_p = NR\eta_{fiber}T\eta_D$ as for the MOT case. The number of atoms turns out to be a very small value

of $N \approx 0.07$, which is 70 times smaller than the number $N \approx 5$ for the MOT case. We have measured the temporal behavior of the peak value by setting the dark period much longer. The decay time is about 4 ms, which is well explained by the free expansion of the MOT cloud. These observations mean that the number of atoms in the observation region has quickly dropped to such a small number during the time interval of 900 ns between switching off the cooling beam and starting the photon counting.

The quick drop may be explained through the following scenario, details of which are discussed elsewhere. Stationary atom number in the observation region is determined by a balance between atom loading to the region and loss in the region. Atoms in the region may finally be adsorbed to the nanofiber surface or reflected back from the surface. Adsorption process acts as the loss process in the observation region and the reflection process as the heating process. Regarding the atom loading, the rate may be much higher with MOT than without MOT beams, because atoms in the MOT are forced to direct towards the trap center due to friction force through cooling beam, whereas atoms without MOT beams are free and simply enter into the observation region just through diffusion.

Present observations have clearly demonstrated the peculiar feature of the nanofiber method to detect a very small number of atoms with high sensitivity. The sensitivity is due to two factors. One is the high coupling efficiency of fluorescence photons to the guided mode. The other is that the nanofiber is immune to the scattering from irradiating light. When we irradiate the nanofiber with probe beam, we readily observe bright light scattering from the nanofiber through a CCD camera. Irradiating photon flux on the nanofiber is estimated to be 2.3×10^{11} photons/s. However, ideally speaking, such scattered radiations cannot couple into the guided mode of the nanofiber, since they are all in radiation modes and are orthogonal to the guided mode. As seen in Fig. 3(b), the observed scattered photon count through the fiber guided mode is very small, 2500 counts/s, which corresponds to a scattering probability of 3.7×10^{-8} . In this meaning, the present nanofiber works almost ideally. Observed scattered photons might be due to some surface irregularities of the nanofiber induced during the nanofiber production and also by dusts on the surface. Such scattering can be reduced much more with further technical advancement.

5. Measurement of fluorescence excitation spectrum through the nanofiber

We measure the fluorescence excitation spectrum of atoms around the nanofiber by scanning the probe laser frequency around the resonance ($6S_{1/2}F = 4 \leftrightarrow 6P_{3/2}F' = 5$). The observed spectrum is displayed in Fig. 4(a) for two probe intensities. We should note that scattering from the probe beam just adds a constant background to the spectrum. The observed line shape is quite different from the usual atomic line shape. No apparent power dependence (broadening) is observed, implying that the spectrum is not due to an isolated atomic spectrum, but consists of many spectral lines overlapped with each other within the spontaneous linewidth. The spectrum reveals a long tail in the red detuned side and consists of two peaks. One peak is almost on the atomic resonance and shows a small red tail. The other peak locates around the detuning $\Delta = -30 \sim -50$ MHz and shows a long red tail up to $\Delta = -140$ MHz. Obviously, these observations are attributed to the van der Waals (vdW) interaction between the Cs-atom and the nanofiber surface which would be dominant for distances closer than $\lambda/2\pi$ from the surface. Since we are observing atoms close to the nanofiber surface, appearance of the vdW interaction should be one of the natural consequences.

The surface-induced red shift of atomic resonance is formulated as $\Delta v_{vdW} \approx v/(k_0 z)^3$, where z is the distance of atom from the surface [10, 11]. Using a parameter $v \approx 0.8$ MHz for Cs-atom and glass surface [10, 11], we calibrate the detuning versus the atom position from the surface as shown in Fig. 4(a). It implies that one can observe atoms which pass through some specific

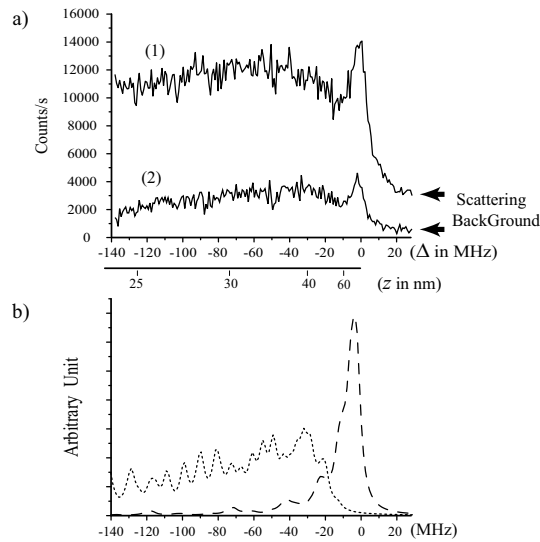


Fig. 4. Excitation spectrum versus probe laser detuning. Detuning Δ is measured relative to atomic resonance. (a) Observed spectrum for two probe intensities; (1) 3.2 mW/cm^2 , and (2) 0.32 mW/cm^2 . Detuning is calibrated to the atom distance z from the surface. (b) Calculated spectrum for the photoassociative transitions (dashed curve) and the bound to bound transitions (dotted curve).

distance from the nanofiber by precisely tuning the probe laser frequency.

In order to clarify the observed spectral shape deeply, we calculate the eigenstates of the center-of-mass motion of the atom in a close vicinity of the nanofiber using known parameters for the vdW potential for the Cs-atom and the silica surface [12]. Calculations are done for the ground and first excited electronic states [13, 14]. As discussed in Ref. [15, 16], the eigenstates are essentially analogous to molecular vibrational states. We calculate the Franck-Condon factors between the ground and excited states and simulate the observable spectral profiles. Regarding the highest bound states, we included up to vibrational states with wavefunction turning point of $z \approx 700 \text{ nm}$. Simulations are carried out for two types of transitions. One is for the transitions from free ground atomic states to the bound vibrational states of the excited vdW potential. This transition corresponds to the photoassociation process; free atoms coming close to the nanofiber transit to the upper bound molecular states, where the molecule consists of the nanofiber and the Cs-atom. The other is for transitions from bound ground vibrational states to bound excited vibrational states. The simulated photoassociation spectral profile is shown in Fig. 4(b) by a dashed curve. The profile is calculated for atoms with velocity distribution at $400 \mu\text{K}$. Upper vibrational states are taken for all possible transitions. The profile is almost on the atomic line with small red tail. Spectral profile for the ground vibrational to excited vibrational states is shown in Fig. 4(b) by a dotted curve. We calculate the profile assuming equal population distribution for ground vibrational states down to a binding energy of 200 MHz . The profile reveals a long red tail with a small offset peak position in the red side. The profile includes more than 100 spectral lines, which are overlapped each other within spontaneous spectral width [13, 14]. We reproduce the observed spectrum with good correspondence by adding the photoassociation and the bound-to-bound profiles with adjusting the relative ratio. Thus we assign the observed red shaded peak on the atomic line as the pho-

toassociation process and the other broad spectrum as due to the bound-to-bound vibrational transitions for atoms in the vdW potential. Note that the spectrum clearly shows the loss mechanism of atoms discussed previously. Since atoms adsorbed in the vdW potential are red-shifted, they are completely out of resonance. Finally, we should mention that the assumption of a pure atomic picture for the atom number estimations is fair enough, since we observe atoms located at about 100 nm away from the fiber surface where the vdW interaction is almost negligible.

6. Summary

In summary, we have demonstrated how optical nanofibers can manipulate and probe atomic fluorescence. We have shown that very small number of atoms, around the nanofiber are detected with a good S/N ratio through single-mode optical fiber under strong resonant laser irradiation. This is essentially due to the particular feature of the optical nanofiber around which an appreciable amount of atomic fluorescence is emitted into the fiber guided mode. The present results imply various possible applications, such as single-atom detection, single-photon generation in an optical fiber or EIT based parametric four-wave mixing [17, 18, 19] using a few atoms around optical nanofibers, which may be of importance in the context of implementing quantum information technologies. Other than the above, the optical nanofiber may have further potential to be used as an efficient tool for quantum optics. Regarding the spatial resolution of atom detection, we should mention that it may be in sub-micrometer scale, since observed fluorescence photons are only from near-surface vdW region as discussed for the excitation spectrum. This high spatial resolution may induce some unique applications in atom optics. The inherent nature of the nanofiber method to detect the vdW interaction between atoms and the surface may open new possible directions to investigate atom-surface interaction with high precision. The optical nanofiber method can naturally be extended to other systems than atoms, like molecules or quantum dots.

Acknowledgments

We are thankful to Manoj Das, Suguru Inoue, Toshiharu Tomonaga, and Jia-Qi Liang for useful discussions and many technical assistances. This work was carried out under the 21st Century COE program on “Innovation in Coherent Optical Science”.